

# An Updated Search of Steady TeV $\gamma$ -Ray Point Sources in Northern Hemisphere Using the Tibet Air Shower Array

(The Tibet AS $\gamma$  Collaboration)

## ABSTRACT

Using the data taken from Tibet II High Density (HD) Array (1997 February-1999 September) and Tibet-III array (1999 November-2005 November), our previous northern sky survey for TeV  $\gamma$ -ray point sources has now been updated by a factor of 2.8 improved statistics. From  $0.0^\circ$  to  $60.0^\circ$  in declination (Dec) range, no new TeV  $\gamma$ -ray point sources with sufficiently high significance were identified while the well-known Crab Nebula and Mrk421 remain to be the brightest TeV  $\gamma$ -ray sources within the field of view of the Tibet air shower array. Based on the currently available data and at the 90% confidence level (C.L.), the flux upper limits for different power law index assumption are re-derived, which are approximately improved by 1.7 times as compared with our previous reported limits.

*Subject headings:* AS $\gamma$  experiment,  $\gamma$ -ray point sources, 90% C.L., flux upper limits

## 1. Introduction

The development of TeV  $\gamma$ -ray observations has experienced a revolutionary progress<sup>[1,2]</sup> since the finish of our northern sky survey work<sup>[3]</sup> (hereafter Paper I). For example, High Energy Stereoscopic System (HESS) experiment alone has discovered more than 40 new  $\gamma$ -ray sources in southern hemisphere with unprecedented angular resolution and sensitivity. Together with other sensitive Imaging Air Cherenkov Telescopes (IACTs), such as Major Atmospheric Gamma Imaging Cherenkov Telescope (MAGIC), Collaboration of Australia and Nippon (Japan) for a GAMMA Ray Observatory in the Outback (CANGAROO), Very Energetic Radiation Imaging Telescope Array System (VERITAS), more than 50 new sources have been discovered in the past several years and the number as well as the diversity of TeV  $\gamma$ -ray sources have been increasing. Spatial and temporal information of these sources are now available with high accuracy and this makes it possible for further studies on acceleration of high-energy cosmic rays, relativistic astrophysics, as well as quantum gravity theory and so forth. To demonstrate the advantage of its wide field of view

and high duty cycle, the Tibet Air Shower Array experiment performed a high-precision measurement on the two-dimensional (2D) anisotropy of cosmic rays in the energy range of a few to several hundred TeV and discovered a fairly compact new anisotropic component in the direction of Cygnus region<sup>[4]</sup>. Furthermore, MILAGRO experiment has discovered an extended  $\gamma$ -ray source in the direction of Cygnus region<sup>[5]</sup> and a few more other sources in the Galactic plane<sup>[6]</sup>, in addition to the diffuse  $\gamma$ -ray emission from the Galactic plane<sup>[7]</sup>. While some of the MILAGRO sources were confirmed or supported by the Tibet Air Shower experiment<sup>[4,8,9]</sup>, it would be extremely interesting and important for the Tibet Air Shower experiment to systematically update its northern sky survey with a much larger data sample currently available.

## 2. Tibet Air Shower Array Experiment and Observations

The Tibet air shower array experiment has been successfully carried out at Yangbajing Cosmic Ray Station (90.522°E, 30.102°N) in Tibet, China, since 1990, at an altitude of 4300m above sea level. Having been upgraded several times<sup>[10,11,12]</sup>, the Tibet HD and III arrays have identical structures except the array size and shape. A 0.5 cm thick lead plate was later placed on top of each counter to improve fast-timing (FT) data by converting  $\gamma$  rays into electron-positron pairs. The angular resolution was first estimated from Monte Carlo (MC) simulations and then confirmed experimentally by observing the Moon shadow to be about  $0.9^\circ$  in the energy range above 3 TeV. The data used in this analysis were collected by running the Tibet HD array for 555.9 live days from 1997 February to 1999 September and the Tibet III array for 1318.9 live days from 1999 November to 2005 November. The events are selected by imposing five criteria on the reconstructed data: (1) Each shower event should fire four or more FT detectors recording 1.25 or more particles. (2) The estimated shower center location should be inside the detector array. (3)  $\sum \rho_{FT}$  should be larger than 15, where  $\sum \rho_{FT}$  is the sum of the number of particles per square meter detected in each detector. (4) The zenith angle of the incident direction should be smaller than  $40^\circ$ . (5) The residual error in direction reconstruction should be less than 1.0m. After applying these cuts and a data quality controll, about  $2.0 \times 10^{10}$  shower events were available for our data analysis here.

## 3. Data Analysis

Based on the successful analysis of Paper I and for simplicity, Method II (i.e., the all-distance “equi-zenith angle” method) was adopted to construct the 2D cosmic ray intensity

map with pixels in the size of  $0.1^\circ \times 0.1^\circ$  in equatorial coordinate. The idea of this method is that at any moment, for all directions, if we scale down (or up) the number of observed events by dividing them by their relative cosmic ray intensity, then those scaled numbers of events in a zenith angle belt should be equal anywhere in the sense of statistics. A  $\chi^2$  function can be built accordingly, the relative intensity of cosmic rays  $I(R.A., Dec)$  and its error  $\Delta I(R.A., Dec)$  in each direction can be solved by minimizing the  $\chi^2$  function. It is worth mentioning that source information in a  $0.1^\circ \times 0.1^\circ$  bin had been included in the intensity  $I(R.A., Dec)$ . For details of this method, the reader is referred to Paper I. To remove the large-scale cosmic ray anisotropy and to keep the local event excess structure which is due to the  $\gamma$ -ray emission, we use the similar subtraction procedure as in Paper I when parameterizing the projected intensity distribution along the right ascension (R.A.) direction for any Dec belt. After subtracting the anisotropy, we can obtain the relative intensity of cosmic rays  $I_{corr}(R.A., Dec)$  and its error  $\Delta I_{corr}(R.A., Dec)$ . The number of excess events and their uncertainties in cell (R.A.,Dec) can be calculated as

$$N_s(R.A., Dec) = [I_{corr}(R.A., Dec) - 1]N_{obs}(R.A., Dec)/I_{corr}(R.A., Dec) \quad (1)$$

$$\Delta N_s(R.A., Dec) = \Delta I_{corr}(R.A., Dec)N_{obs}(R.A., Dec)/I_{corr}(R.A., Dec) \quad (2)$$

where  $N_{obs}(R.A., Dec)$  is the number of events in an on-source bin.

Given the angular resolution of the Tibet air shower array, events are summed up from a cone with an axis pointing to the source direction, and the half-opening angle is set as  $0.9^\circ$  (for  $E > 3\text{TeV}$ )<sup>[13]</sup> or  $0.4^\circ$  (for  $E > 10\text{TeV}$ ). All celestial cells with their centers located inside the cone contribute to the number of events as well as its uncertainty. Finally, the significance for an on-source window centered at the cell  $(R.A._{on}, Dec_{on})$  can be calculated by

$$S(R.A._{on}, Dec_{on}) = \frac{\sum_{(R.A., Dec) \in cone} \{[I_{corr}(R.A., Dec) - 1]N_{obs}(R.A., Dec)/I_{corr}(R.A., Dec)\}}{\sqrt{\sum_{(R.A., Dec) \in cone} [\Delta I_{corr}(R.A., Dec)N_{obs}(R.A., Dec)/I_{corr}(R.A., Dec)]}} \quad (3)$$

The systematic uncertainty for the significance value due to the above subtraction procedure on large-scale anisotropy is estimated to be  $0.2\sigma$  by adjusting the bin size and the smoothing parameters.

## 4. Results and Conclusions

Distribution of significance for all bins in the surveyed sky are shown in Fig.1. It agrees very well with a normal distribution on the negative side, indicating that systematic

effects are well under control. The positive side contains more high-significance entries than those expected from pure statistical fluctuations, and they are related to two well-known TeV  $\gamma$ -ray sources, namely the Crab Nebula and Mrk421. After removing their contributions, in such a way that those cells within  $2^\circ$  regions around the Crab Nebula and Mrk421 are excluded, we get the dash-dotted histogram as shown in Fig.1, consistent with the expectations from random background fluctuations.

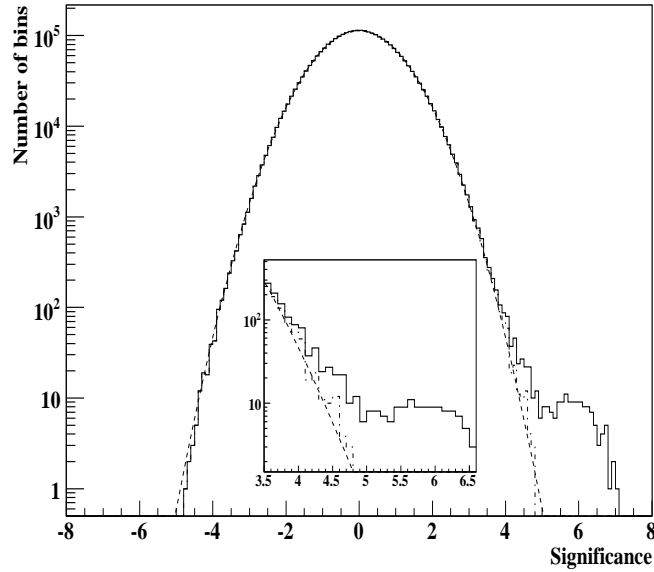


**Fig.1** The significance map is shown here. The solid curve is derived from all cells defined in the analysis. The dash-dotted histogram excludes cells close to the Crab Nebula or Mrk421. The dashed line represents the best fit of a Gaussian curve to the data, its mean is  $-0.002 \pm 0.01$  and standard deviation is  $1.013 \pm 0.005$ .

For our updated sky survey, the information of five candidates for possible  $\gamma$ -ray sources, each with an excess of greater than  $4.5\sigma$ , are summarized in Table 1. Only the pixel with the highest significance from each independent direction is listed.

As can be seen in Table 1, the list includes two established sources Crab Nebula and Mrk421 which remain to be the brightest TeV  $\gamma$ -ray sources in the northern sky. Compared with Paper I, the significance of the Crab Nebula is increased from  $5.0\sigma$  to  $7.1\sigma$  at the highest significance position (from  $4.1\sigma$  to  $6.0\sigma$  at the nominal position of the Crab Nebula, which is consistent with the expected enhancement from  $3.7\sigma$  to  $6.2\sigma$  within error bars according to the changing statistics); while the significance of Mrk421 is dropped somewhat mainly

Table 1: Candidate locations of all directions with an excess greater than  $4.5\sigma$

No.	<i>R.A.</i>	<i>Dec</i>	$N_{ON}$	$N_{OFF}$	$N_S$	$\Delta N_S$	$S_{pretrials}$
1	57.95	53.25	2405072.8	2397926.7	7146.1	1548.5	4.6
2	70.55	11.35	2306840.6	2299785.4	7055.2	1516.5	4.7
3 <sup>a</sup>	83.75	21.95	3078848.1	3066434.9	12413.3	1751.1	7.1
4	89.45	30.05	3359526.5	3350799.7	8726.8	1830.5	4.8
5 <sup>b</sup>	166.25	38.25	3301780.3	3292945.8	8834.4	1814.6	4.9

**Table 1** The columns are (from left to right) sequence of prominent direction, R.A.(J2000), Dec(J2000), number of measured events in on-source window ( $N_{ON}$ ), number of background events ( $N_{OFF}$ ), event number excess in on-source window ( $N_S = N_{ON} - N_{OFF}$ ), uncertainty on the event number excess ( $\Delta N_S$ ), and the significance  $S_{pretrials}$  of deviation  $N_{ON}$  from  $N_{OFF}$ .

**Notes:** R.A. and Dec columns are due to the way we divide the bin in the analyses; 3<sup>a</sup>—The Crab Nebula and 5<sup>b</sup>—Mrk421.

due to the fact that Mrk421 is not a stable source; it happens to be in a high state with the data used in Paper I but remains less active<sup>[14]</sup> in the succeeding period when the data are used in the current analysis. As for the other two candidates in Table 1, No.2 and No.4 have also appeared in Paper I; however their significance values are slightly decreased after we have included more data into this analysis. There are still two other sources located at  $(70.45^\circ, 18.05^\circ)$  and  $(221.75^\circ, 32.75^\circ)$  which passed in Paper I but failed this time, and the current analysis selects a new candidate at position  $(57.95^\circ, 53.25^\circ)$  with a significance value just above  $4.5\sigma$ . It should be noted that the above-discussed phenomena, except the Crab Nebula and Mrk421, are probably due to the background fluctuations and also possibly due to their intrinsic unstable features; the conclusive results will rely on a further data analysis. In summary, compared with Paper I, the number of hot spots reduces from 4 to 3 (only for the candidates determined from Method II and by excluding the two known sources: the Crab Nebula and Mrk421). Both are consistent with the expectation from statistic fluctuation. With 200 Toy MC experiments, the numbers of hot spots(each satisfies  $4.5\sigma$  requirement) are obtained for each experiment, the probabilities to observe no less 4 and 3 are found to be 8% and 26% respectively. In addition, the locations of candidates are somewhat different between the two observations. As for the difference, it agrees with the pointing accuracy of the Tibet AS $\gamma$  array. Taking Crab Nebula ( $0.4^\circ$  position difference between two observations) as an example, we estimate the probability with MC experiments and find 40% of the MC experiments have a position difference no less than  $0.4^\circ$ . Nevertheless, given the large number of trials, the significance values from all directions other than the Crab Nebula and Mrk421 are not high enough to definitely claim any existence of a new point source, although they will become clearer with the future improved statistics of observational data

or can be interesting regions for further follow-up observations with more sensitive IACTs.

It is worth mentioning that the two MILAGRO newly reported TeV sources, MGRO J1908+06<sup>[6]</sup> and MGRO J2019+37<sup>[5]</sup> not listed in Table 1 due to their lower significance, had been our two candidates with only marginal yet persistent event excess. In Paper I, we found  $4.8\sigma$  on  $(286.65^\circ, 5.55^\circ)$ ,  $0.4^\circ$  angular separation from MGRO J1908+06. However the significance value is  $4.3\sigma$  in the current analysis, not scaled up with the increase of statistics but consistent with the expectation based on the flux measured by MILAGRO<sup>[6]</sup> and HESS<sup>[15]</sup>. Another interesting point source, close to an extended source MGRO J2019+37, has been discussed several times in Tibet AS $\gamma$  papers<sup>[4,16,17]</sup>. Our dedicated analysis has reported a preliminary  $5.8\sigma$  excess in  $(304^\circ, 36.1^\circ)$ <sup>[9]</sup> and this result should be regarded as a confirmation of the MILAGRO’s discovery<sup>[2]</sup>. While less sensitive to such an extended source, the current point source search analysis still finds a  $4.0\sigma$  excess in the direction of  $(303.25^\circ, 35.95^\circ)$ .

Based on the above analysis we know that the significance from all directions other than the Crab Nebula and Mrk421 are not high enough to definitely claim any existence of a new point source, we set a 90% C.L. upper flux limit for all directions in the sky, except at the positions of the Crab Nebula and Mrk421. The prescription of Helene<sup>[18]</sup> is used to calculate the upper limits of the number of signal events at the 90% C.L. for energies higher than 3TeV and 10TeV from each region of the northern sky. Then the effective detection area of the Tibet air shower array is evaluated by full MC simulation assuming a Crab-like  $\gamma$ -ray spectrum  $E^{-2.6}$  for a set of Dec values ( $0.0^\circ, 10.0^\circ, 20.0^\circ, 30.0^\circ, 40.0^\circ, 50.0^\circ$ , and  $60.0^\circ$ ) and interpolated to other Dec values between  $0.0^\circ$  and  $60.0^\circ$ . Taking into account the live time, the newly derived 90% C.L. average flux upper limit along the R.A. direction as a function of Dec is shown in Fig. 2(a), which is  $(0.8 \sim 1.9) \times 10^{-12} \text{ cm}^{-2} \text{ s}^{-1}$  for  $E > 3\text{TeV}$  and  $(1.3 \sim 2.5) \times 10^{-13} \text{ cm}^{-2} \text{ s}^{-1}$  for  $E > 10\text{TeV}$  respectively. Additionally, since the response of the Tibet air shower array is energy dependent, the flux upper limits obtained from these data are dependent on the energy spectra of the possible sources of TeV gamma rays. The same procedure is applied to the cases of other power-law indices for energy above 3TeV and 10TeV, the corresponding average flux limits can be found in Fig.2(b), which are  $(0.8 \sim 2.2) \times 10^{-12} \text{ cm}^{-2} \text{ s}^{-1}$  for  $E > 3\text{TeV}$  and  $(1.2 \sim 3.0) \times 10^{-13} \text{ cm}^{-2} \text{ s}^{-1}$  for  $E > 10\text{TeV}$  respectively and have approximately 1.7 improvement compared with the reported limits in Paper I. These limits are well consistent with the fact that the majority of  $\gamma$ -ray sources discovered in recent years have integrated fluxes less than 10% of those of the Crab Nebula at 1TeV energy<sup>[19]</sup>.

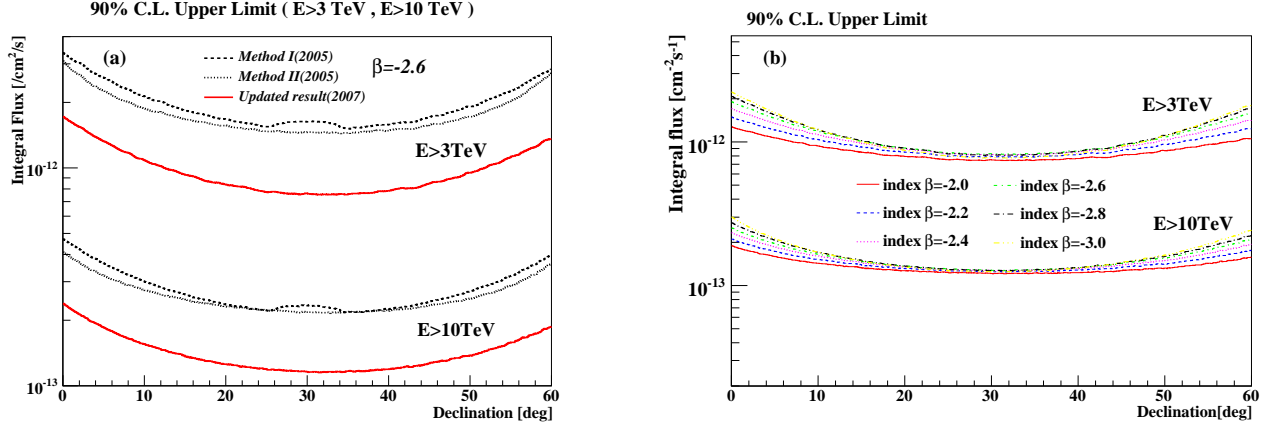


**Fig.2** R.A. direction-averaged 90% C.L. upper limit on the integral flux above 3TeV and 10TeV. **(a)** for a Crab-like point source, i.e., with an energy spectrum of  $E^{-2.6}$ ; **(b)** for different indices of power-law spectra.

In conclusion, we performed an updated northern sky survey for the TeV  $\gamma$ -ray point sources in a Dec band between  $0.0^\circ$  and  $60.0^\circ$  using about eight-year data obtained from February 1997 to November 2005 by the Tibet air shower array. The significance except Crab and Mrk421 is not high enough to definitely claim any existence of new sources. Accordingly, more stringent 90% C.L. flux upper limits than the ones in Paper I are set from the rest of positions based on the assumption that candidate point sources have power-law spectra with indices varying from 2.0 to 3.0. In the near future, we will add a large muon detector array under the Tibet air shower array for the purpose of increasing its  $\gamma$ -ray sensitivity in the 100 TeV energy region (10-1000 TeV) by discriminating between  $\gamma$  rays and the cosmic-ray hadrons<sup>[20]</sup>. According to a full MC simulation, flux sensitivity of this new project will be an order or more better than the present one in the 100TeV region<sup>[21]</sup>. Approximately 10 new sources are expected to be discovered and we will be able to measure the cutoff energies of known and unknown sources which are potential origins of Galactic cosmic rays.

The collaborative experiment of the Tibet Air Shower Arrays has been performed under the auspices of the Ministry of Science and Technology of China and the Ministry of Foreign Affairs of Japan. This work is supported in part by Grants-in-Aid for Scientific Research on Priority Areas (712) (MEXT), by the Japan Society for the Promotion of Science (JSPS), by the National Natural Science Foundation of China (in part by NSFC Grants 10675134 and 10533020) and by the Chinese Academy of Sciences.

## REFERENCES

- Aharonian, F. A., *Science* 2007, **315**: 70
- Hinton, J., *arXiv:0712.3352v1 [astro-ph]* 2007
- Amenomori, M., Ayabe, S., et al. *ApJ* 2005, **633**: 1005 (Paper I)
- Amenomori, M., Ayabe, S., et al. *Science* 2006, **314**: 439
- Abdo, A. A., Allen, B., et al. *ApJ* 2007, **658**: 33
- Abdo, A. A., Allen, B., et al. *ApJ* 2007, **664**: 91
- Atkins, R., Benbow, W., et al. *Phys. Rev. Lett.* 2005, **95**: 251103
- Zhang J.L. for the Tibet AS $\gamma$  Collaboration *28th ICRC* 2003, **4**:2405
- Amenomori, M., Bi, X.J., et al. *30th ICRC* 2007, (in press)
- Amenomori, M., Ayabe, S., et al. *ApJ* 2003, **598**: 242
- Amenomori, M., et al. *PRD*. 1993, **47**: 2675
- Amenomori, M., et al. *27th ICRC* 2001, **2**: 573
- Chen Xin, Zhou Xun-Xiu, et al. *High Energy Physics and Nuclear Physics*, 2004, **28**: 1094
- [http://xte.mit.edu/ASM\\_lc.html](http://xte.mit.edu/ASM_lc.html)
- Djannati-atai, A., Ona-wilhelmi, E., *30th ICRC* 2007, (in press)
- Amenomori, M., Ayabe, S., et al. *27th ICRC* 2001, **6**: 2544
- Cui, S.W., Yan, C.T., et al. *28th ICRC* 2003, **4**: 2315
- Helene, O. *Nucl. Instrum. Methods Phys. Res.* 1983, **212**: 319
- Casanova, S., Dingus, B. L., *arXiv:0711.2753v2 [astro-ph]* 2007
- Amenomori, M., Ayabe, S., et al. *Astrophysics and Space Science* 2007, **309**: 435
- Amenomori, M., Bi, X.J., et al. *30th ICRC* 2007, (in press) (arXiv:0710.2757 [astro-ph])